Electronic Supplementary Material (ESI) for RSC Advances.

Supplementary Information

Solute-Particle Separation in Microfluidics Enhanced by Symmetrical Convection

Yurou Yao[1], Yao Lin[1], Zerui Wu[1], Zida Li[2], Xuemei He[3], Yun Wu[3], Zimin Sun[3*], Weiping Ding[4*] and Liqun He[1*]

1. Department of Thermal Science and Energy Engineering, University of Science and Technology of China, Hefei 230026, China.

2. Department of Biomedical Engineering, Medical School, Shenzhen University, Shenzhen 518060, China.

3. Department of Hematology, The First Affiliated Hospital of University of Science and Technology of China, Hefei 230001, China

4. Department of Electronic Engineering and Information Science, University of Science and Technology of China, Hefei 230026, China.

* Corresponding addresses: zmsun@ustc.edu.cn, wpdings@ustc.edu.cn, heliqun@ustc.edu.cn

The flow channel depth of the mass transfer section in all models used in this paper is 0.1 mm, and the two-dimensional dimensional drawings of each model are shown in Fig. S1.

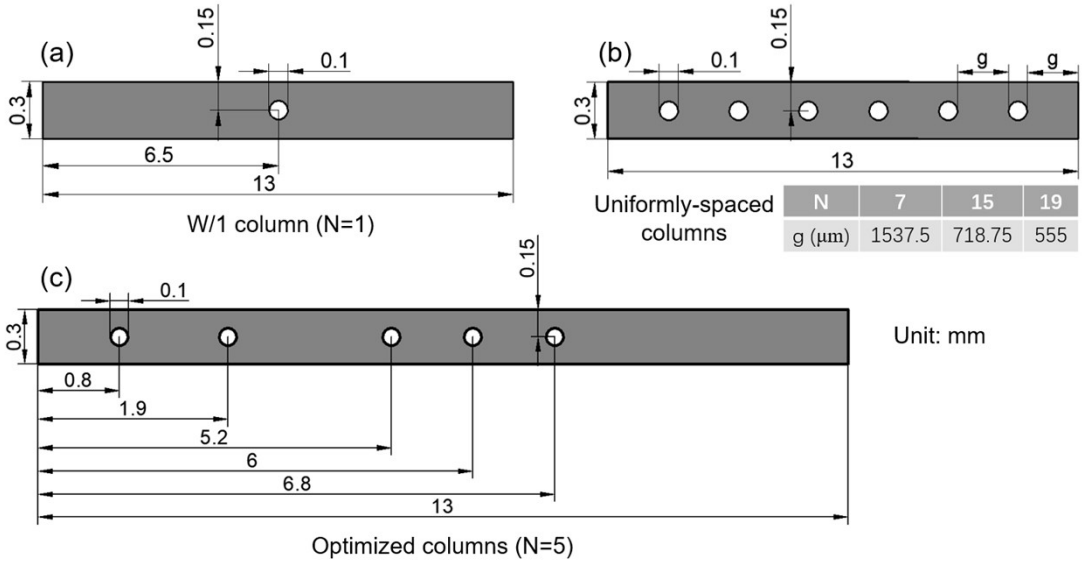

Fig. S1 Dimensions of the model mass transfer section. (a) Model with one column. (b) Model with uniformly-spaced columns. (c) Model with optimized columns.

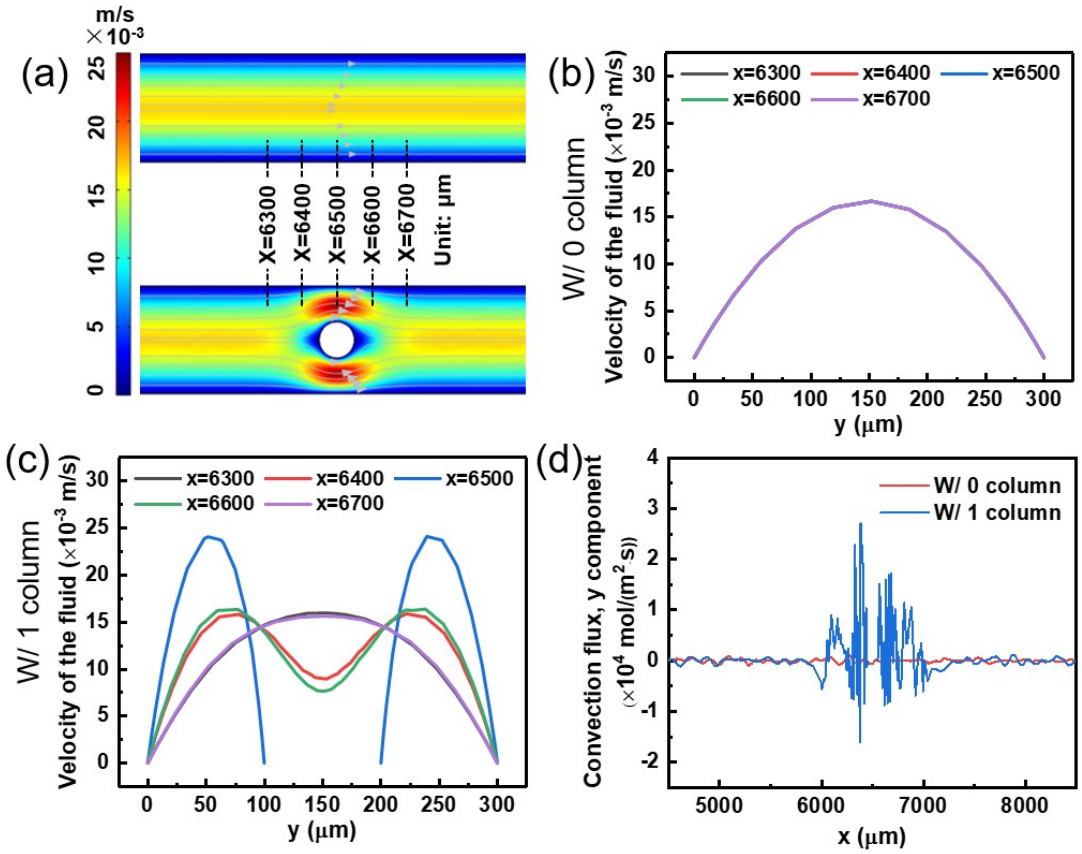

Fig. S2 Effect of column on fluid flow. (a) Simulation results of the velocity distribution in the flow channel before and after adding the column. (b) Changes in fluid velocity at different locations along the width of the flow path in the model without column. (c) The variation of fluid velocity at different locations along the width of the flow path in the model with one column. (d) The y-direction component of the convective mass transfer flux between the two fluids before and after the addition of the column varies with the length of the flow path, and the positive direction is from the blood side to the dialysate side.

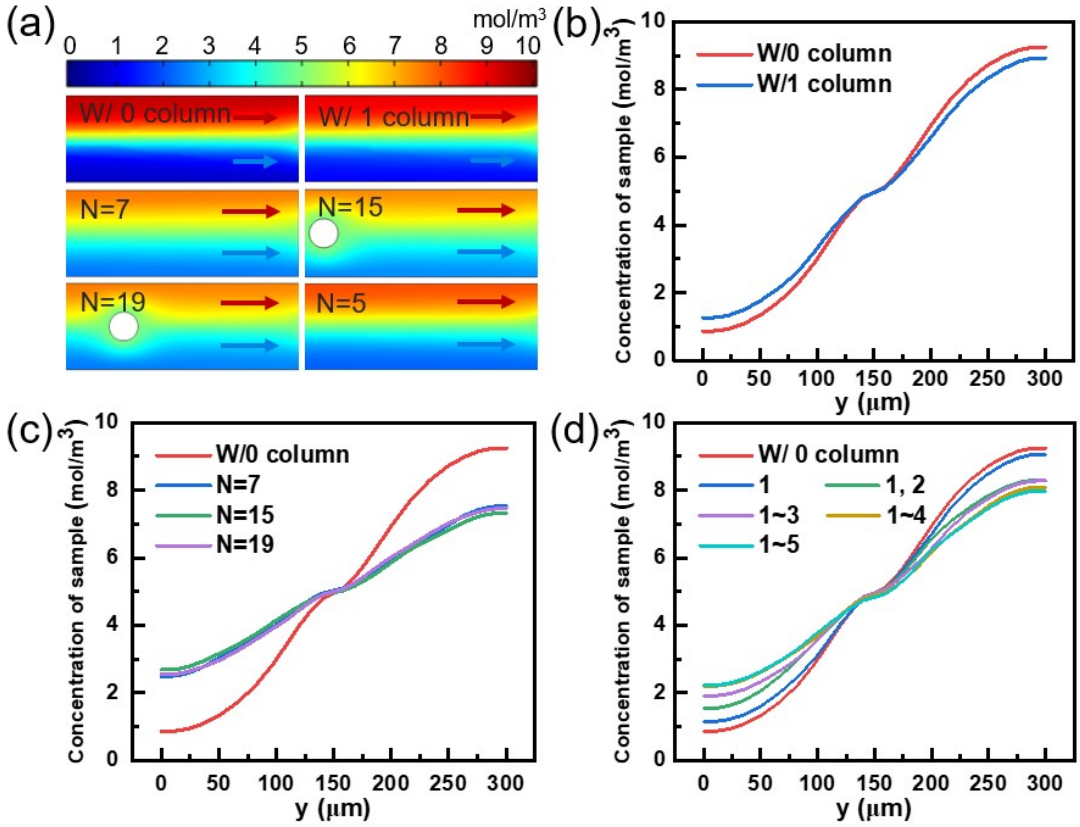

Fig. S3 Concentration distribution at the outlet of mass transfer section of different models. (a) Simulation results of concentration distribution near the outlet of mass transfer sections of different models. (b) Mass transfer section of model without/ with a column. (c) Mass transfer section of model without column and with different column spacing. (d) Columnless model and optimized model with columns added one by one.

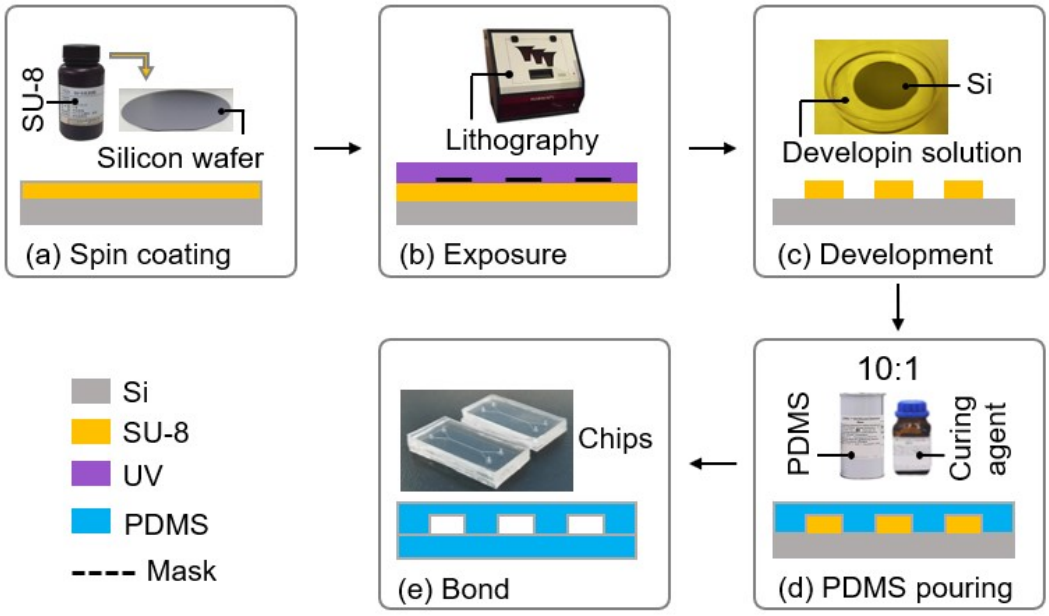

Fig. S4 Manufacturing flow chart of microfluidic chip. (a) Spin-coating SU-8 photoresist onto the silicon wafer (Thickness of 0.1 mm). (b) UV exposure to pattern the SU-8 coated silicon wafer. (c) Develop the exposed silicon wafer with developer. (d) Pour PDMS on the patterned silicon wafer. (e) Demould and bond the PDMS.

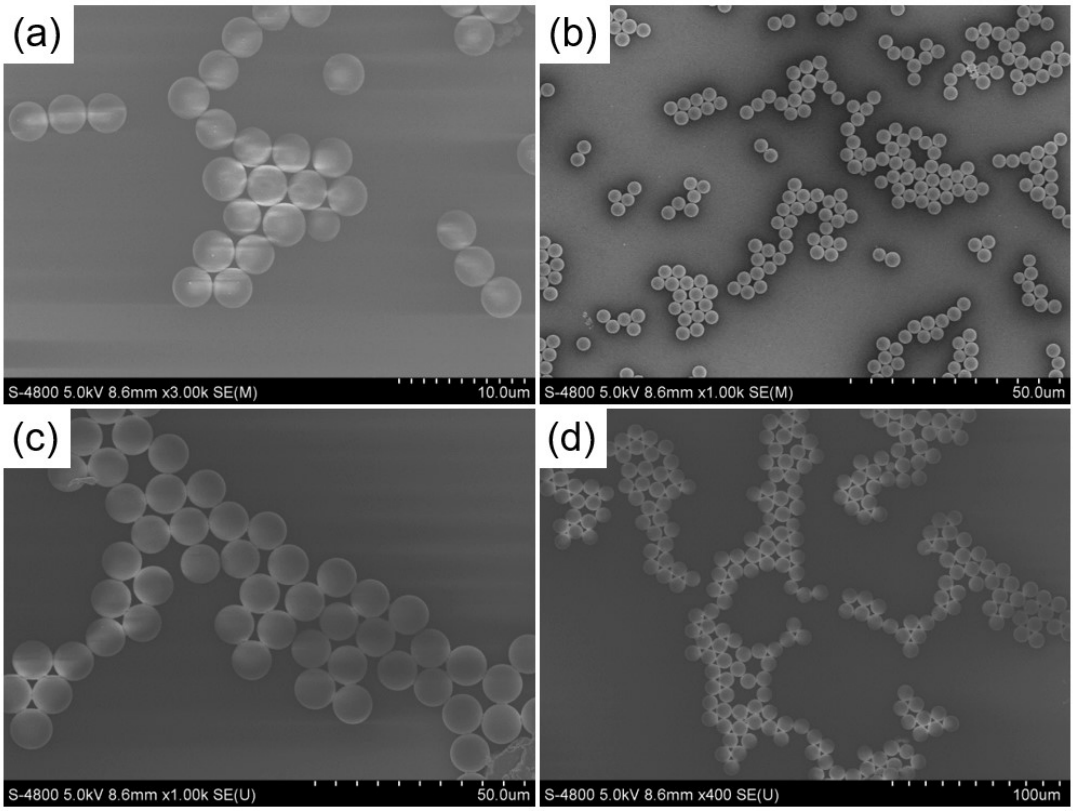

Fig. S5 Scanning electron microscopy of polymethyl methacrylate (PMMA) microsphere dispersion. (a) and (b) are 3 μm microsphere dispersions magnified 3000 and 1000 times, respectively; (c) and (d) are 10 μm microsphere dispersions magnified 1000 and 400 times, respectively.

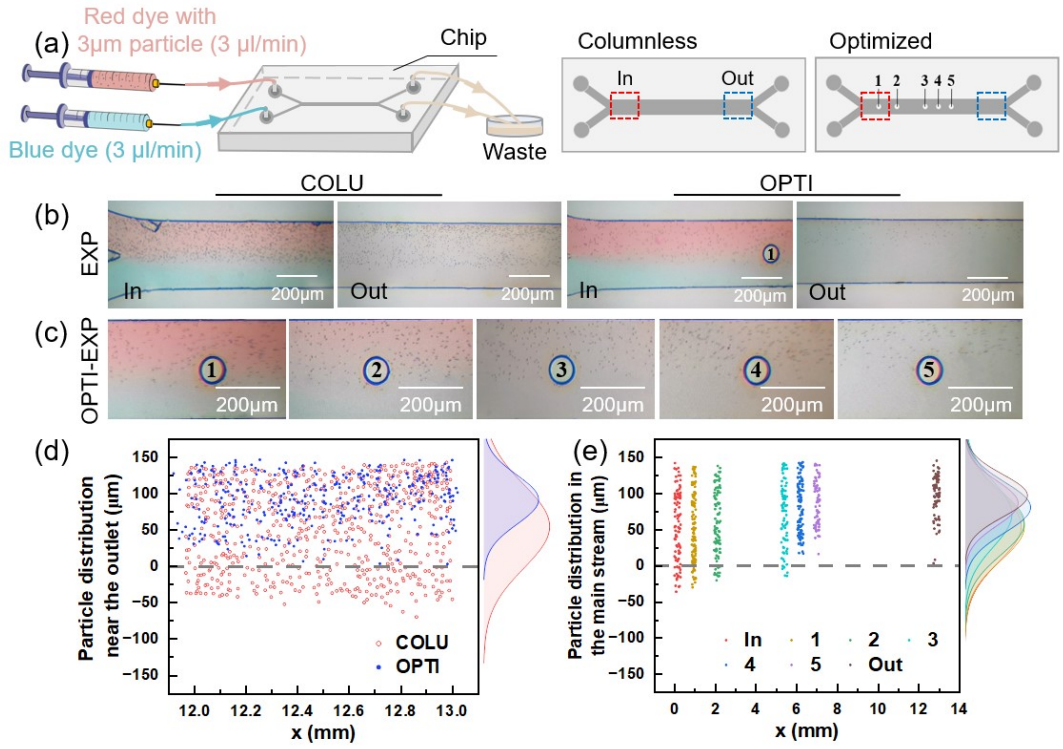

Fig. S6 Interception of 3 μm microspheres by column array. (a) Schematic diagram of the experimental setup. (b) Distribution of 3 μm microspheres in two chips near the inlet and outlet of the main flow channel. The scale bars denote 200 μm. (c) Distribution of 3 μm microspheres in the optimized chip near each column. The scale bars denote 200 μm. (d) Distribution pattern of 3 μm microspheres in the outlet of two chips. (e) Distribution pattern of 3 μm microspheres along the main channel of the optimized chip.

Fig. S6(d) shows the distribution of 3 μm microspheres near the outlet of the columnless chip and the optimized chip. For the outlet of the columnless model, the peak density of the 3 μm microspheres is 75.81 μm (y direction) from the center of the flow channel, and the distribution range of the microspheres is -69.88 ~ 142.53 μm. after adding the column array, the peak density is located at 91.45 μm, which is shifted 15.64 μm toward the side wall, and the distribution range of the microspheres is reduced to 3.07 ~ 146.21μm.

Fig. S6(e) shows the distribution of 3 μm microspheres near the inlet and outlet of the optimized chip and 300 μm after each column. The peak density of microspheres near the inlet is at 54.61 μm from the center of the flow channel with a distribution range of -35.91 ~ 142.14 μm, and after passing through the five columns sequentially, the peak density of microspheres is located at 54.06, 59.13, 71.42, 77.73, and 79.32 μm,

moving toward the sidewalls by -0.55, 4.52, 16.81, 23.12, and 24.71 μm, with microsphere distributions ranging from -29.87 ~ 136.99, -20.1 ~ 138.24, -14.15 ~ 141.29, 6.69 ~ 143.43, and 16.16 ~ 141.04 μm, respectively. The peak density near the final outlet is at 96.29 μm, moving 41.68 μm toward the sidewall compared to the inlet, with the main distribution of microspheres range is 3.45 ~ 145.52 μm.

The smaller diameter and higher concentration of the 3 μm spheres are more likely to diffuse laterally, and microspheres that have moved to the water side before flowing to the column cannot be intercepted by the column, so they may cause a small amount of loss.